CERN-TH/2000-289
hep-ph/0010044

Higher-order QCD corrections to $\gamma^*\gamma^* \to hadrons$ [1]

Stefano Frixione[a]

[a]CERN, TH division, Geneva, Switzerland

I illustrate the techniques and the results of the computation of order-α_S corrections to the production of hadrons in the collision of two virtual photons, that originate from the incoming leptons at e^+e^- colliders.

1. Introduction

In the study of scattering phenomena in the limit of very large energies at fixed momentum transfer, one must face the fact that the two most promising probes of BFKL physics, namely small-x effects in DIS and large-rapidity-gap events in dijet production at hadron colliders, are inherently dependent upon long-distance physics, due to the presence of hadrons in the initial state; this poses serious difficulties on the possibility of cleanly extracting signals of BFKL physics from data.

To overcome these difficulties a gedanken experiment has been proposed [1], where two quarkonium states collide; the transverse size of the quarkonium is small enough to allow the perturbative computation of its wave function. Of course, since quarkonium colliders are out of sight, one must devise some other solutions; an increasing-popular one is the study of the process

$$\gamma^* + \gamma^* \longrightarrow hadrons, \tag{1}$$

at fixed photon virtualities $-q_i^2 = Q_i^2 > 0$, and for large center-of-mass energies squared $W = (q_1+q_2)^2$; here, we denote with q_i the momenta of the photons. The virtual photons play the same role as the quarkonia; they are colourless, and their virtualities control their transverse sizes, which are roughly proportional to $1/\sqrt{Q_i^2}$, thus allowing for a completely perturbative treatment. Notice that the virtuality of the photon is therefore physically equivalent to the (squared) mass of the quarkonium; however, while the mass of the quarkonium is fixed by nature, the virtuality of the photon can be controlled by the experimental setup.

[1]Talk given at QCD00, 6-12 July 2000, Montpellier, F.

The easiest way to access the process of eq. (1) is through the following reaction:

$$e^+ + e^- \quad \longrightarrow \quad e^+ + e^- + \underbrace{\gamma^* + \gamma^*}_{\longrightarrow\, hadrons;} \tag{2}$$

namely, one considers e^+e^- collisions, selecting those events in which the incoming leptons produce the photons through the elementary $e^+e^-\gamma$ vertex, and the two photons eventually initiate the hard scattering that produces the hadrons. Data relevant to the process in eq. (2) have been published by several experiments in the past, and many more are expected in the near future by LEP collaborations; it goes without saying that a linear collider would be the ideal place where to look at such processes.

It is clear that the process in eq. (2) is non physical; rather, it has to be understood as a shorthand notation for a subset of Feynman diagrams contributing to the process that is actually observed:

$$e^+ + e^- \longrightarrow e^+ + e^- + hadrons. \tag{3}$$

Other contributions to the process in eq. (3) are, for example, those in which the incoming e^+e^- pair annihilates into a photon or a Z, eventually producing hadrons and a lepton pair, or those in which one (or both) of the two photons in eq. (2) is replaced by a Z. However, it is not difficult to devise a set of cuts such that the process in eq. (2) gives the only non-negligible contribution to the process in eq. (3). One can tag *both* the outgoing leptons, and retain only those events in which the scattering angles of the leptons are small: in such a way, the contamination due to annihilation processes is safely negligible. Furthermore,

small-angle tagging also guarantees that the photon virtualities are never too large (at LEP2, one typically measures $Q_i^2 = \mathcal{O}(10\ \mathrm{GeV}^2)$; therefore, the contribution from processes in which a photon is replaced by a Z is also negligible. Thus, it is not difficult to extract the cross section of the process $\gamma^*\gamma^* \to hadrons$ from the data relevant to the process in eq. (3).

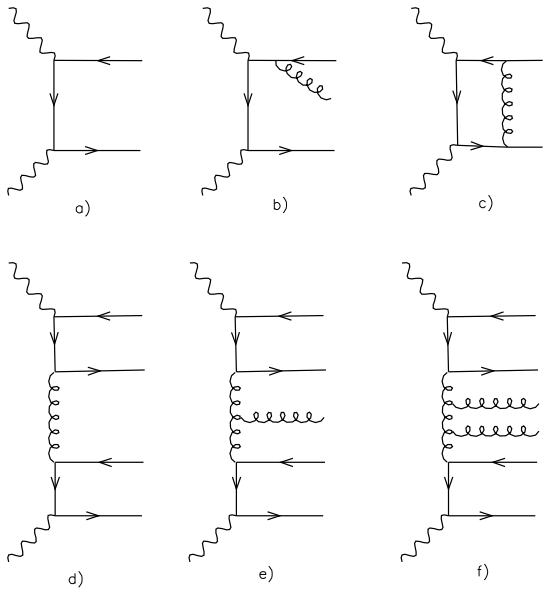

Figure 1. Sample of diagrams contributing to the production of hadrons in two-photon collisions.

Eventually, the data are compared to the theoretical predictions obtained by using BFKL equation. Some of the diagrams contributing to the process in eq. (1) are depicted in fig. 1; diagrams d), e) and f) (plus all the diagrams obtained by emitting more and more gluons from the t-channel gluon) are included in BFKL dynamics. In the large-W limit, diagrams with a t-channel quark exchange, such as a), b) and c), are expected to give a cross section behaving as

$$\sigma_{\gamma^*\gamma^*} \sim 1/W, \qquad (4)$$

while diagrams relevant to BFKL physics, such as d), e) and f), are expected to give

$$\sigma_{\gamma^*\gamma^*}^{BFKL} \sim 1 + \sum_{j=1}^{\infty} a_j (\alpha_S L)^j + \mathcal{O}(\alpha_S (\alpha_S L)^j), \qquad (5)$$

where $L = \log(W/\mu_{\mathrm{w}}^2)$ is a "large" logarithm, and all subleading logarithmic terms are indicated with $\mathcal{O}(\alpha_S(\alpha_S L)^j)$; the quantity μ_{w}^2 is a mass scale squared, of the order of the photon virtualities. By comparing eqs. (4) and (5), it is clear that the latter will dominate over the former in the asymptotic energy region $W \to \infty$. However, at current collider energies, $\sigma_{\gamma^*\gamma^*}$ is not safely negligible, and must be taken into proper account when comparing theory and data. For this reason, one usually *subtracts* the theoretical predictions for $\sigma_{\gamma^*\gamma^*}$ from data, and then compares the results obtained in this way to the predictions for $\sigma_{\gamma^*\gamma^*}^{BFKL}$. Unfortunately, at present only the leading order contribution (diagram a) in fig. 1) to $\sigma_{\gamma^*\gamma^*}$ has been considered. This amounts to say that diagrams such as b) and c) have been neglected so far; these diagrams represent the first non-trivial QCD corrections to the process in eq. (1). We will denote these contributions as next-to-leading order (NLO) corrections, although effectively of leading order in α_S. The aim of this work, which presents preliminary results from ref. [2], is to report the computation of these NLO corrections.

2. Computation of NLO corrections

The computation of the NLO corrections to a hard scattering process is by now a rather standard procedure, since algorithms exist that are universal (that is, process independent), and applicable to any number of final state partons. The role of these algorithms is to combine in a physically sensible way the virtual and the real contributions, that are unphysical and divergent upon loop and phase-space integrations. The information on the hard process basically enter only in the computation of the matrix elements. In our case, one needs to compute the amplitude of the process $e^+e^- \to e^+e^- q\bar{q}$ at one loop, and of the process $e^+e^- \to e^+e^- q\bar{q}g$ at the tree level. Fortunately, these results are easily obtained from ex-

isting literature (notice that we work with massless flavours; being mainly interested in the region of W not close to the heavy-quark threshold, our approximation is sufficiently good). As far as the one-loop amplitude is concerned, we can derive it from the one-loop amplitude relevant to the process $e^+e^- \to q_a\bar{q}_a q_b\bar{q}_b$ given in ref. [3]. For the tree-level amplitude, we can use the results of ref. [4] relevant to the process $q\bar{q} \to Z^*Z^*g \to l_a\bar{l}_a l_b\bar{l}_b g$, with a suitable crossing and inserting the electromagnetic coupling factors instead of the electroweak ones; the fact that the Z has an axial coupling is easily dealt with, since the results of ref. [4] are given in terms of helicity amplitudes.

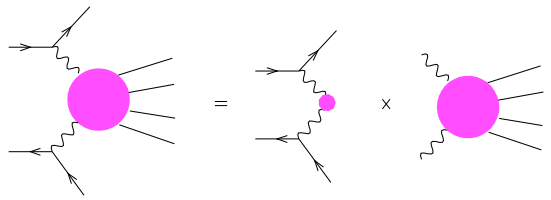

Figure 2. Decomposition of the phase space for the process $e^+e^- \to e^+e^- + hadrons$.

Having the matrix elements at disposal, one can plug them is his preferred NLO algorithm, and get physical results. Our case can however be greatly simplified in a preliminary stage; in fact, the incoming and outgoing leptons actually do not participate in the hard scattering, that is initiated by the two virtual photons. Formally, the simplification goes through a suitable decomposition of the phase space, which is pictorially represented in fig. 2. We write the phase space of two leptons plus n partons (in our case, $n = 2$ or $n = 3$ for the one-loop or the tree-level amplitudes respectively) as follows

$$d\Phi_{2+n}(p_1+p_2;p_1',p_2',k_1,\ldots,k_n) = d\Gamma(p_1',p_2')d\Phi_n(q_1+q_2;k_1,\ldots,k_n), \quad (6)$$

where p_i (p_i') and $q_i = p_i - p_i'$ are the momenta of the incoming (outgoing) leptons and photons respectively, and k_i are the momenta of the final state (coloured) partons. The first entry in $d\Phi_{2+n}$ and $d\Phi_n$ is the sum of the momenta of the incoming particles (the e^+e^- pair and the two-photon pair respectively, as shown in fig. 2). Eq. (6) implicitly defines $d\Gamma$, since we know *a priori* how to write the phase space for an arbitrary number of particles, given their momenta. We can thus immediately get

$$d\Gamma = \frac{d^3p_1'}{(2\pi)^3 2p_1'^0}\frac{d^3p_2'}{(2\pi)^3 2p_2'^0}. \quad (7)$$

We have therefore decomposed the original phase space into the product of two pieces, each of which is Lorentz invariant. We exploit this fact by rewriting eq. (7) in the center-of-mass frame of the incoming e^+e^- pair: defining $S = (p_1+p_2)^2$, we get

$$d\Gamma = \frac{1}{4(2\pi)^6 S} dQ_1^2 dQ_2^2 dE_1 dE_2 d\varphi d\bar{\varphi}, \quad (8)$$

where φ and $\bar{\varphi}$ are two generic azimuthal angles, one of which (let's say φ to be definite) can be interpreted as the angle between the two outgoing leptons; E_i are the energies of the outgoing leptons in the center-of-mass frame of the incoming e^+e^- pair. The strategy of the computation should now be clear. The hard process that we actually deal with at NLO is that of eq. (1); thanks to the decomposition in eq. (6), we have a $2 \to n$ phase space which is formally identical to that one gets as a starting point of any NLO algorithm; thus, we can safely adopt one of the existing NLO algorithms, and study the process of eq. (1) in the $\gamma^*\gamma^*$ center-of-mass frame, without any reference to the incoming or outgoing leptons: this amounts to a non-trivial simplification, since the complexity of the numerical computations at NLO is known to grow fast with the number of particles involved in the hard scattering. Of course, the information on the lepton momenta is entering somewhere, in particular in the matrix elements; to take into account this fact, we proceed in two steps, still using fig. 2 as a guide. We start by generating the full kinematical configuration of the outgoing leptons, using eq. (8). In

doing this, we also get the photon momenta, and therefore we know how to boost from the e^+e^- to the $\gamma^*\gamma^*$ center-of-mass frame. Then, we boost the lepton momenta to the $\gamma^*\gamma^*$ center-of-mass frame, where we generate the remaining (parton) momenta, according to the phase space $d\Phi_n$; at this point, we can perform all the manipulations required by the NLO algorithm.

3. Results

Following the procedure outlined in the previous section, we constructed a user-friendly code capable of predicting, to NLO accuracy, any infrared-safe quantity constructed with up to three partons (plus two leptons) in the final state.[2] The code is based upon the NLO algorithm of refs. [5,6], and it is a suitable modification of one of the codes presented in ref. [6].

In order to produce phenomenological results, we used the following input parameters, taken from an analysis performed by L3 [7]; we stress that other physically sensible sets of parameters would lead to the same qualitative conclusions. The center-of-mass energy is fixed to $\sqrt{S} =$ 200 GeV; the scattering angles θ_i and energies E_i of the outgoing leptons are required to fulfill $0.03 \leq \theta_i \leq 0.066$ and $E_i > 40$ GeV, respectively (actually, L3 use $E_i > 30$ GeV; we prefer a slightly larger value in order to have larger virtualities. The relative difference between the two choices is of the order of 1%). We use a two-loop expression for α_S, with $\alpha_S(M_Z) = 0.1181$ [8]. A choice has also to be made for the scales entering the strong and electromagnetic running coupling constants. For the latter, we left the possibility open in the code to have independent scales for the two photon legs; it seems therefore natural to choose each scale equal to the virtuality of the corresponding leg. As far as the scale entering the strong coupling is concerned, we have chosen

$$\mu^2 = \frac{Q_1^2 + Q_2^2}{2} + \left(\frac{\sum_{i=1}^n k_{Ti}}{2} \right)^2, \tag{9}$$

where k_{Ti} are the transverse momenta (in the $\gamma^*\gamma^*$ center-of-mass frame) of the emitted coloured partons; a discussion on this choice will be given in ref. [2].

In fig. 3 we present our results for the total cross section in e^+e^- collisions (that is, relevant to the process in eq. (2)), as a function of Y. This quantity is defined as follows:

$$Y = \log(S/S_0), \quad S_0 = \frac{\sqrt{Q_1^2 Q_2^2}}{y_1 y_2}, \tag{10}$$

where

$$y_i = 1 - \frac{2E_i}{\sqrt{S}} \cos^2(\theta_i/2). \tag{11}$$

It is worth noticing that Y is directly related to the BFKL logarithm L entering eq. (5). In fact, for large W's, $W \simeq y_1 y_2 S$; furthermore (see for example ref. [9]), a sensible choice is $\mu_{\rm w}^2 = c_Q \sqrt{Q_1^2 Q_2^2}$, with c_Q a suitable constant. It then follows that

$$L = Y - \log c_Q. \tag{12}$$

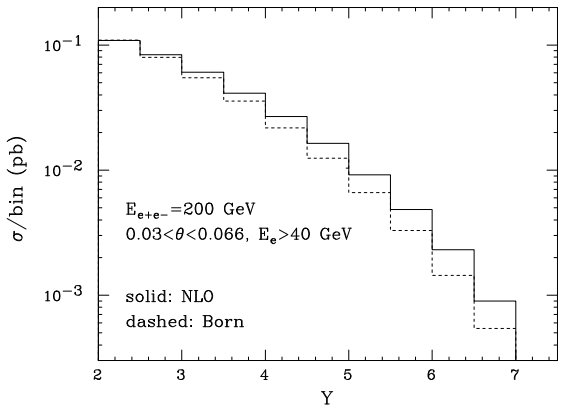

Figure 3. Cross section as a function of Y. The LO and NLO results are both shown.

In fig. 3, the dashed histogram represents the LO result, while the solid histogram is the full NLO result; thus, the difference between the two histograms is the order-α_S correction computed

[2]The code can be obtained upon request by mailing to Stefano.Frixione@cern.ch.

in this paper. As can be seen from the figure, the NLO corrections are basically negligible when small Y's are considered. On the other hand, in the region of intermediate and large Y, the NLO corrections are definitely more important; at $Y = 4$ ($Y = 6$), the LO result is increased by a factor of about 1.2 (1.6). This is a non trivial piece of news; in fact, when comparing L3 data to LO predictions at – say – $Y = 4$, theory underestimates the data by a factor of about 2.5. This fact is interpreted as the signal of a dominant contribution coming from diagrams with a t-channel gluon exchange. However, the result given here shows that part of the discrepancy has to be associated with diagrams that do not have any t-channel gluon exchange. In other words, the BFKL asymptotic region is probably still far away, and this implies that the contributions of diagrams with four quarks (that is, of order α_S^2), but without t-channel gluons, is probably not completely negligible. In any case, for a precise comparison between theory and data, NLO corrections cannot be ignored.

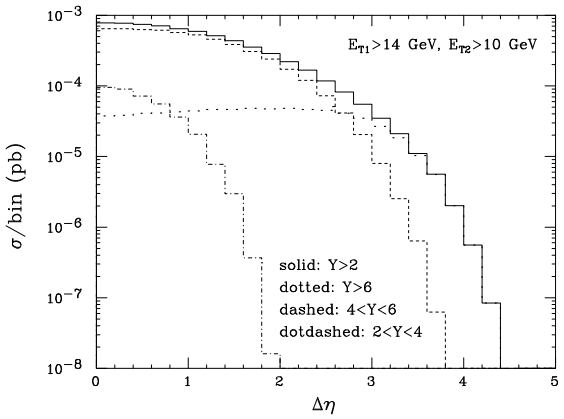

Figure 4. Dijet cross section at NLO.

We now go back to eq. (12), and consider the role of the constant c_Q. In ref. [9], this constant has been estimated by equating the definition of L with the rapidity difference between the most forward and backward quarks produced in the hard scattering. We can repeat the same exercise, using jets instead of quarks (as one always should, when a NLO computation is available). We thus computed two-jet cross sections, selecting the most forward/backward jets and requiring the most (least) energetic of them to have transverse energy larger than 14 (10) GeV in the center-of-mass frame of the $\gamma^*\gamma^*$ pair. The difference in their rapidities, denoted as $\Delta\eta$, is shown in fig. 4, for various cuts on Y. It is interesting to notice that the contribution due to the large Y region (dotted histogram, corresponding to $Y > 6$) basically coincides, in the large $\Delta\eta$ region, with the cross section integrated over all Y's. We therefore find what we expect, namely that the large Y region is basically populated by events characterised by two hard jets well separated in rapidity. Thus, following ref. [9], we can invert eq. (12) to get c_Q, by substituting $Y = 6$ and identifying L with the average $\Delta\eta$ corresponding to the cut $Y > 6$. We have

$$c_Q = \exp(Y - \langle\Delta\eta\rangle) \simeq 75, \tag{13}$$

which is rather close to the value of 100 estimated in ref. [9]. The author wishes to thank Vittorio Del Duca for reading the manuscript.

REFERENCES

1. A.H. Mueller, *Nucl. Phys.* **B415**(1994)373; A.H. Mueller and B. Patel, *Nucl. Phys.* **B425**(1994)471.
2. M. Cacciari, V. Del Duca, S. Frixione and Z. Trocsanyi, in preparation.
3. Z. Bern, L. Dixon and D.A. Kosower, *Nucl. Phys.* **B513**(1998)3.
4. L. Dixon, Z. Kunszt and A. Signer, *Nucl. Phys.* **B531**(1998)3.
5. S. Frixione, Z. Kunszt and A. Signer, *Nucl. Phys.* **B467**(1996)399.
6. S. Frixione, *Nucl. Phys.* **B507**(1997)295.
7. L3 Collaboration, M. Acciarri *et al.*, *Phys. Lett.* **B453**(1999)333.
8. D.E. Groom *et al.*, *Eur. Phys. J.* **C15**(2000)1.
9. S.J. Brodsky, F. Hautmann and D.E. Soper, *Phys. Rev. Lett.* **78**(1997)803; *Phys. Rev.* **D56**(1997)6957.